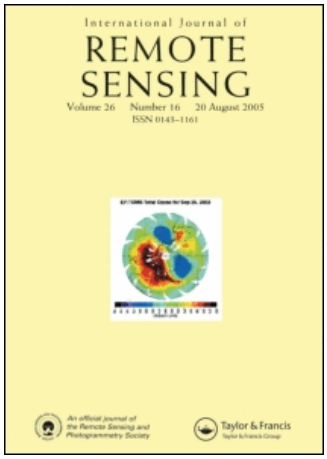

International Journal of Remote Sensing
Publication details, including instructions for authors and subscription information:
http://www.informaworld.com/smpp/title~content=t713722504

Impact of rainfall anomalies on Fourier parameters of NDVI time series of northwestern Argentina

M. M. González Loyarte [a]; M. Menenti [b]

[a] Instituto Argentino de Investigaciones de las Zonas Áridas (IADIZA/CRICYT), Consejo Nacional de Investigaciones Científicas y Técnicas, 5500 Mendoza, Argentina
[b] Istituto per i Sistemi Agricoli e Forestali del Mediterraneo - ISAFoM, 80040 S. Sebastiano al Vesuvio, Italy

Online Publication Date: 01 February 2008

To cite this Article: Loyarte, M. M. González and Menenti, M. (2008) 'Impact of rainfall anomalies on Fourier parameters of NDVI time series of northwestern Argentina', International Journal of Remote Sensing, 29:4, 1125 — 1152

To link to this article: DOI: 10.1080/01431160701355223
URL: http://dx.doi.org/10.1080/01431160701355223

International Journal of Remote Sensing
Vol. 29, No. 4, 20 February 2008, 1125–1152

Impact of rainfall anomalies on Fourier parameters of NDVI time series of northwestern Argentina

M. M. GONZÁLEZ LOYARTE*† and M. MENENTI‡

†Instituto Argentino de Investigaciones de las Zonas Áridas (IADIZA/CRICYT), Consejo Nacional de Investigaciones Científicas y Técnicas, PO Box 507, 5500 Mendoza, Argentina

‡Istituto per i Sistemi Agricoli e Forestali del Mediterraneo – ISAFoM, Casella Postale 101, 80040 S. Sebastiano al Vesuvio, Italy

(*Received 22 April 2005; in final form 17 March 2007*)

This paper describes a method to detect the impact of rainfall anomalies on vegetation phenology, in terms of timing (phase) and greenness, by using Fourier series to fit a time series of Normalized Difference Vegetation Index (NDVI) observations. The study was conducted in the northern semiarid region of Argentina, where rainfall is the driving factor of vegetation phenology. A 9-year time series of monthly NDVI Global Area Coverage (GAC) images, obtained with the National Oceanic and Atmospheric Administration (NOAA) Advanced Very High Resolution Radiometer (AVHRR), was split into nine series of 12-monthly images, each corresponding to a yearly growth cycle. A Fast Fourier Transform (FFT) algorithm was applied to each cycle, and derived parameters were analysed according to rainfall anomalies for irrigated and rainfed crops, grasslands and native forest. Derived Fourier parameters were: mean NDVI, amplitude and phase. Both negative and positive rainfall anomalies had a significant impact on the Fourier parameters. Amplitude and phase were the most sensitive parameters. Droughts modified the monomodal structure of the yearly cycle by decreasing the contribution of the 12-month periodic component and increasing the contribution of the 6-month component. The impact of drought on the Fourier parameters was highest for rainfed crops. Yearly values of Fourier parameters for grasslands and native forest were affected by prevailing hydrological conditions over the previous year.

1. Introduction

The study of types of vegetation cover, phenology and climate conditions by applying National Oceanic and Atmospheric Administration (NOAA) Advanced Very High Resolution Radiometer (AVHRR) Normalized Difference Vegetation Index (NDVI) imagery at the regional scale has been successful (Justice *at al*. 1985, 1986, Townshend and Justice 1986). Potter and Brooks (1998) explained 70–80% of the spatial variability in the NDVI seasonal extremes for different plant functional types through climate indices based on temperature and rainfall.

Henricksen and Durkin (1986) demonstrated that the start and end of the growing season in Ethiopia, assessed with NDVI images, were strongly associated with a moisture index. The time-integrated NDVI for each growing season was also found

*Corresponding author. Email: gloyarte@lab.cricyt.edu.ar

International Journal of Remote Sensing
ISSN 0143-1161 print/ISSN 1366-5901 online
http://www.tandf.co.uk/journals
DOI: 10.1080/01431160701355223

to be closely correlated with rainfall for the Sudanese savanna (Hielkema *et al.* 1986). A strong linear relationship was found between NDVI and annual rainfall in the range 150–1000 mm for the western Sahel (Malo and Nicholson 1990). Recently, Anyamba and Tucker (2005) expanded the analysis of NDVI data on Sahelian vegetation dynamics as a proxy for the response of land surface to rainfall variability for the period 1981–2003, and detected drought and 'wetter' conditions that were in agreement with the recent region-wide trends in rainfall. Justice *et al.* (1991) found a general relationship between rainfall estimates from Meteosat data and NOAA-AVHRR NDVI, where the time lag between rainfall and NDVI was particularly notable on sites where rainfall was the limiting factor for growth.

Several authors have demonstrated the usefulness of NOAA-AVHRR NDVI to detect the effect of droughts in both Ethiopia (Henricksen 1986, Henricksen and Durkin 1986) and Sahel (Tucker *et al.* 1986). NOAA-AVHRR NDVI series have also been used to study the interannual variability produced by El Niño–Southern Oscillation (ENSO) events (Liu and Negrón Juárez 2001, Seiler and Kogan 2002, Gurgel and Ferreira 2003, Poveda and Salazar 2004). Liu and Negrón Juárez (2001) were able to model high anomaly values of NDVI and ENSO indices to predict the onset of drought in northeastern Brazil 4 months in advance with 68% success.

Rainfall variability and its effect on phenology was documented by Menenti *et al.* (1991, 1993), who developed a methodology to map isogrowth zones of Africa and South America (Azzali and Menenti 1996). A measure of the 'quality' of vegetation zones in dynamic terms is obtained by using the Fast Fourier Transform (FFT) of NDVI time series.

The FFT algorithm used in this study enables us to decompose, for every pixel, the temporal profile of the NDVI series in an average signal plus $N/2$ sinusoidal components, with N being the length of the time series expressed as the number of images (Menenti *et al.* 1993, Azzali and Menenti 1996). The average signal is the mean NDVI value for the whole time series of observations, and periodic (sinusoidal) components are characterized by amplitude and phase. In this paper all of these parameters, the mean NDVI, and the amplitude and phase for every period are referred to as Fourier parameters. Amplitude and phase are associated with a given period; 12 and 6 months in our analysis. The amplitude value represents a measurement of the maximum variability of NDVI at a given period, and the phase is the time lag between this maximum and the initial point of the series. The decomposition of a complex time series of NDVI images into simpler periodic signals has enabled an understanding of the relative weights of different periodic climate processes such as rainfall and temperature on both vegetation complexes (Azzali and Menenti 2000) and foliar seasonality (Fuller and Prince 1996) in Southern Africa.

An FFT approach similar to that used for Southern Africa (Azzali and Menenti 2000) was also used to monitor variability of vegetation cover in Argentina (González Loyarte 1996) and to analyse the regional climate in northeastern Brazil as well as the annual NDVI cycle (Negrón Juárez and Liu 2001). Roerink *et al.* (2003) reported that Fourier components, mean NDVI and yearly amplitude, are sensitive indicators of climate variability. Negrón Juárez and Liu (2001) concluded that the phase image was useful to distinguish spatial and seasonal rainfall variations in northeast Brazil. Other applications have been reported by Moody and Johnson (2001), who used the discrete Fourier transform on a 7-year NDVI series to map land cover types in southern California, and by Jakubauskas *et al.* (2001), who

applied the Harmonic analysis (Fourier) to 26 biweekly NDVI data from a single year for crop-type identification in southwestern Kansas.

Droughts, being negative rainfall anomalies, affect vegetation cover, biomass and phenology, and these characteristics can be studied at a regional level by analysing time series of NOAA-AVHRR NDVI data. Fourier parameters derived from an NDVI time series are useful to describe and summarize foliar rhythms and their interannual variability.

Several research questions need to be answered: (i) How useful are Fourier parameters in the detection of rainfall anomalies, particularly droughts, over a certain period? (ii) To what extent do Fourier parameters provide a sensitive measure of rainfall anomalies? (iii) Do all parameters respond equally to rainfall anomalies? (iv) How are these parameters modified under positive and negative rainfall anomalies? These questions guided this study.

The area selected to study these questions is the province of Santiago del Estero, a plain in the semi-arid zone of northwestern Argentina with rainfall between 300 and 800 mm (Roig *et al.* 1988) (figure 1(*a*)). Due to the interannual variability of rainfall

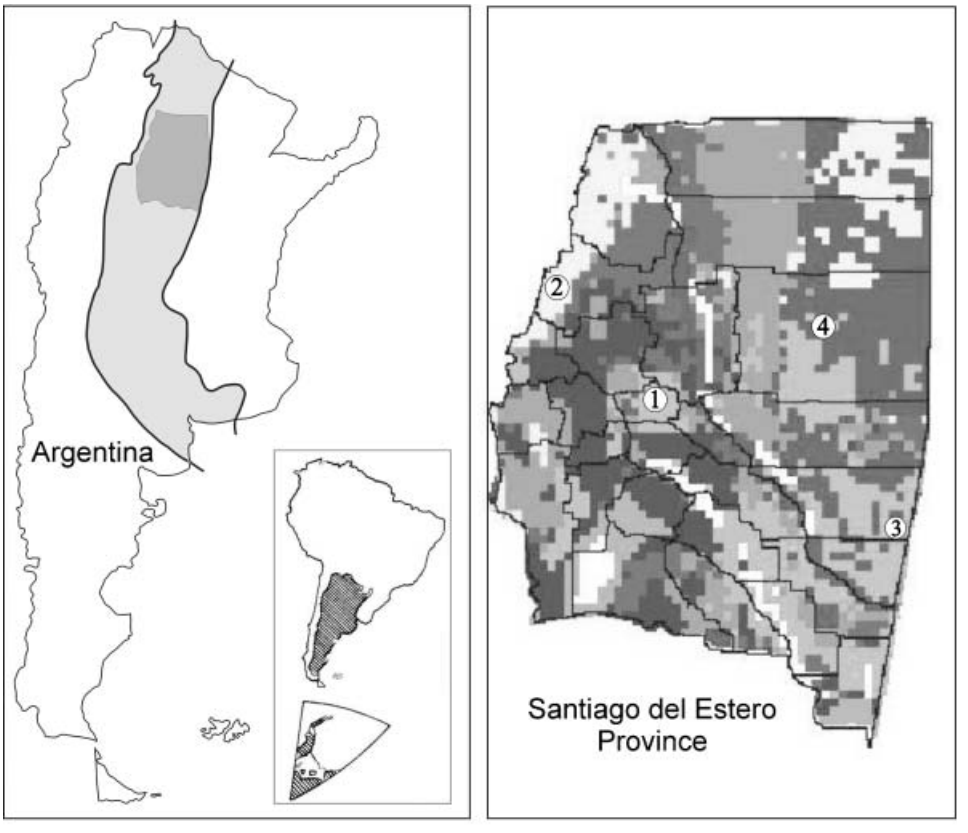

Figure 1. Study area. (*a*) Location of the Santiago del Estero Province (dark grey) in the northern semi-arid zone of Argentina (light grey). (*b*) Land use map from González Loyarte and Menenti (2000) and location of associated meteorological stations: 1, Santiago del Estero (irrigated crops); 2, Pozo Hondo (rainfed crops); 3, Bandera (grasslands); 4, Tintina (native forest).

(Minetti and Sierra 1984, Le Houérou 1999), this region is at risk of drought. Drought was defined by Bobba de González and Minetti (2001) as rainfall below the historical average (1941–90). Minetti and Bobba de González (1998) calculated an Annual Regional Drought Index (ARDI) with a theoretical maximum index of 12. During the period of time spanned by observations used in this study (1982–91), they detected a drought for 1988–89 with an ARDI of 8. This drought affected a wider region in northwest Argentina and all major ecosystems (Bobba de González and Minetti 2001), consistent with a La Niña event in Argentina (Seiler and Kogan 2002).

Positive rainfall anomalies occurred in northern Argentina during the 1970s (Minetti and Sierra 1984, Hoffmann 1988), and some areas became temporarily subhumid and humid (González Loyarte 1995). Annual rainfall averages of the decades 1971–80 and 1981–90 for Santiago del Estero province are above the 50-year historical average (1941–90) (Minetti and Acuña 1997). The northern part of Argentina is influenced by the Atlantic semipermanent anticyclone (Bruniard 1982), with rain in spring and summer, under a quasi-monsoon regime (Poblete *et al*. 1989). The mean annual temperature at Santiago del Estero Station (20.7°C) is not a limiting factor for life, the driving factor of vegetation growth is rainfall (Bianchi and Yañez 1992). Thus, the droughts having the strongest impact on vegetation are those occurring during the growing season (Minetti and Bobba de González 1998), that is the humid period of the year from September to May (spring to autumn) when 96% of rainfall occurs.

The aim of this study was to evaluate the response of Fourier parameters to rainfall anomalies using a time series of NOAA-AVHRR NDVI data in 'natural' and agricultural environments in the semi-arid region of Argentina (Santiago del Estero province) for nine yearly growth cycles.

2. Study area and data set

2.1 *Selected land cover types*

Based on a land cover map (González Loyarte and Menenti 2000), four land cover types were selected: (1) irrigated crops, (2) rainfed crops, (3) grasslands and (4) native forest. These are considered reference vegetation types because of their expected contrasting responses to rainfall variability. Each of them was associated with a meteorological station for rainfall analyses: Santiago del Estero, Pozo Hondo, Bandera and Tintina, respectively (figure 1(*b*)). Bandera station corresponds to a warm, dry–subhumid climate, and the others to a hot semi-arid climate (Torres Bruchmann 1981).

The dominant land cover type in the province of Santiago del Estero is the dry forest of the Chaco region, which is the most uninterrupted and largest dry forest in South America (Hueck 1978). The forest is widespread; from extended forests with different degrees of exploitation to narrow strips of woodlands mostly for protection of patches of rainfed and irrigated crops and grasslands, or isolated trees in the midst of grasslands to provide shade to cattle.

Irrigated crops are fully (99.4%) associated with the dam of Río Hondo for the supply of water delivered by the Dulce river. The image samples selected for the analysis belong to the Robles Department, which produces mainly vegetables, cotton, maize and annual and perennial forage. In the irrigated area, vegetation cover is a sequence of cultivated plots larger than 5 ha, combined with narrow strips

of the remaining forest for protection of croplands, with the cultivated area being dominant. Among the horticultural crops, representing 46% of the cropland area, the most important are: onions, tomato, zucchini, sweet potato (figure 2(*a*)), lettuce, and carrot. Among the industrial crops, cotton is dominant and occupies 19% of the area (figure 2(*b*)). Maize is dominant among cereals, with 16% of the total croplands (figure 2(*c*)). Perennials are dominant among forage species, with alfalfa covering 10% of the cropland area (figure 2(*d*)). The above-mentioned crops cover 91% of cropland in the Robles Department. In the woodland strips, trees are not higher than 12 m; about 40–50% of the vegetation is perennial, with evergreen trees and shrubs, reaching 100% cover with spring–summer rains.

The rainfed crop sample is in the Jiménez Department and belongs to the new boundary of rainfed agriculture. This is due to the positive climate fluctuation during the 1970s and 1980s, which encouraged intensive deforestation to cultivate rainfed crops. In the study area around Pozo Hondo Station, cultivated rainfed patches are larger than 10 ha and are limited by strips of remaining open forest accounting for less than 10% of the total cropland (figure 3). Among the rainfed crops, soya bean is dominant (55%) (figure 3(*a*)), followed by sorghum (15%), bean (14%) and maize (5%); 11% of the total rainfed cropland is devoted equally to annual and perennial forage crops (figure 3(*b*)) (INDEC 1989).

The grassland class in the Belgrano Department is the result of the expansion of the boundary of the livestock area, that is of the Pampean zone. For the whole

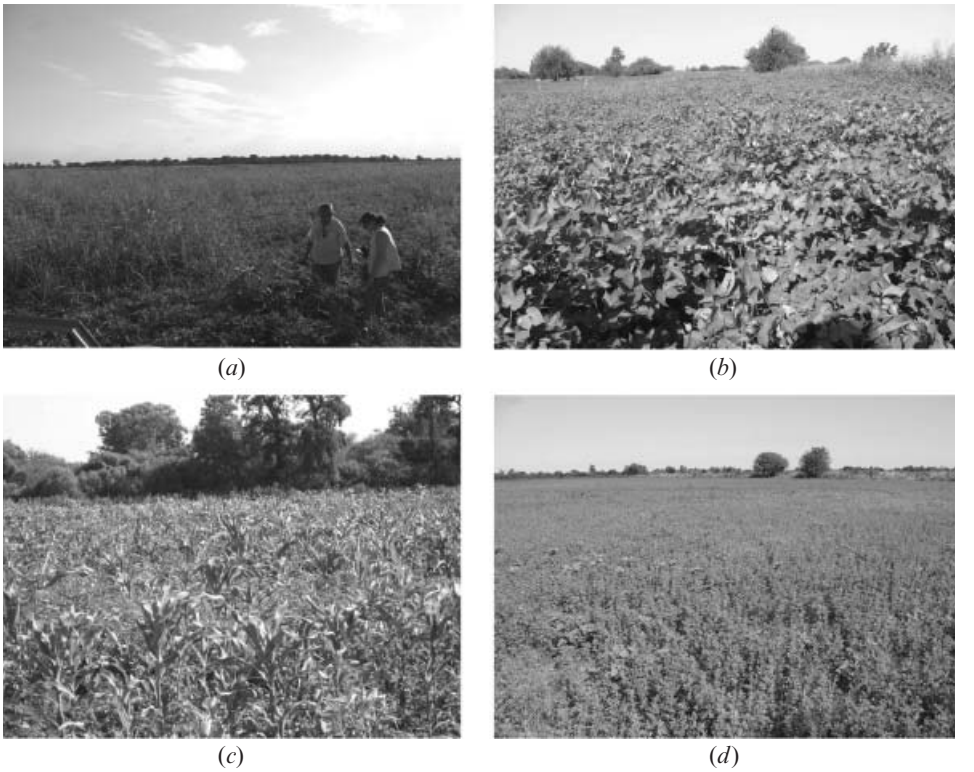

Figure 2. Irrigated area. (*a*) Sweet potato ready for harvesting. (*b*) Cotton plantation at fruit stage. (*c*) Maize. (*d*) Three-year-old alfalfa with 6–7 harvests a year. Los Robles Department, Santiago del Estero Province, Argentina.

(*a*) (*b*)

Figure 3. Rainfed area. (*a*) Soya bean at fully expanded trifoliate leaf stage. (*b*) Area devoted to forage. Jiménez Department, Santiago del Estero Province, Argentina.

region, 52% of the area is covered mostly with natural grasslands dominated by perennial species, whereas artificial grasslands are composed equally of annuals and perennials. There are also some fodder crops (4%) such as sorghum, rye and barley, and 41% is woodland (INDEC 1989). Around Bandera Station, strips of remaining open forest cover about 30% of the area on the edge of grasslands (figure 4(*a*)) and crop fields; among the crops, sorghum is dominant (77%) (figure 4(*b*)). The woodland is an open forest with the tree layer reduced to 20–40% cover by intensive use. *Aspidosperma quebracho-blanco* and *Schinopsis lorentzii* are the species in the upper layer, and the lower tree layer is composed mainly of *Prosopis* spp, *Acacia aromo* and *Cercidium australe* (figure 4(*c*)).

The native forest class (Chaco forest) is dominant (75%) in the Moreno Department, where forest exploitation is the dominant activity. Around Tintina location, the landscape is dominated by the forest, only interrupted by roads, settlements (villages) and small patches of grassland, mainly around isolated settlements ('puestos') (figure 5(*a*)). This is a broadleaf forest with two layers of trees with a total cover of 50–70%. The upper layer (up to 16–20 m) is composed of *A. quebracho-blanco* ('quebracho blanco') and *S. lorentzii* ('quebracho colorado santiagueño') (figure 5(*b*)). The lower tree layer (7–10 m) is composed mostly of *Zizyphus mistol*, *Acacia aromo*, *Prosopis kuntzei*, *Cercidium praecox*, *Prosopis nigra* and *Caesalpinia paraguariensis* (figure 5(*c*)). Fractional soil cover of *Prosopis* species around settlements is above 50% (figure 5(*d*)). Regarding leaf persistence, *A. quebracho-blanco* is evergreen, and the second species in order of importance, *S. lorentzii*, is deciduous but loses its leaves at the end of winter, a short time before the spring rainfall starts. As regards the second tree layer, *P. kuntzei* has small leaves lasting only 1 month, its abundant branches and thorns are green and photosynthetically active; *Z. mistol* keeps its leaves for almost all the year. Therefore, the forest foliage is almost always green throughout the year, whereas shrubs and herbaceous layers mainly follow the phenological rhythm of dryness in winter. According to Ledesma and Ledesma (1983), this forest combines the high and intermediate tree layers with brush and grass layers, where species are broadleaved, deciduous and evergreen, so as to keep the soil covered all year round. Soils are clay or silt with a high capacity of water retention, which provides a greater water supply to trees and shrubs than to grasses.

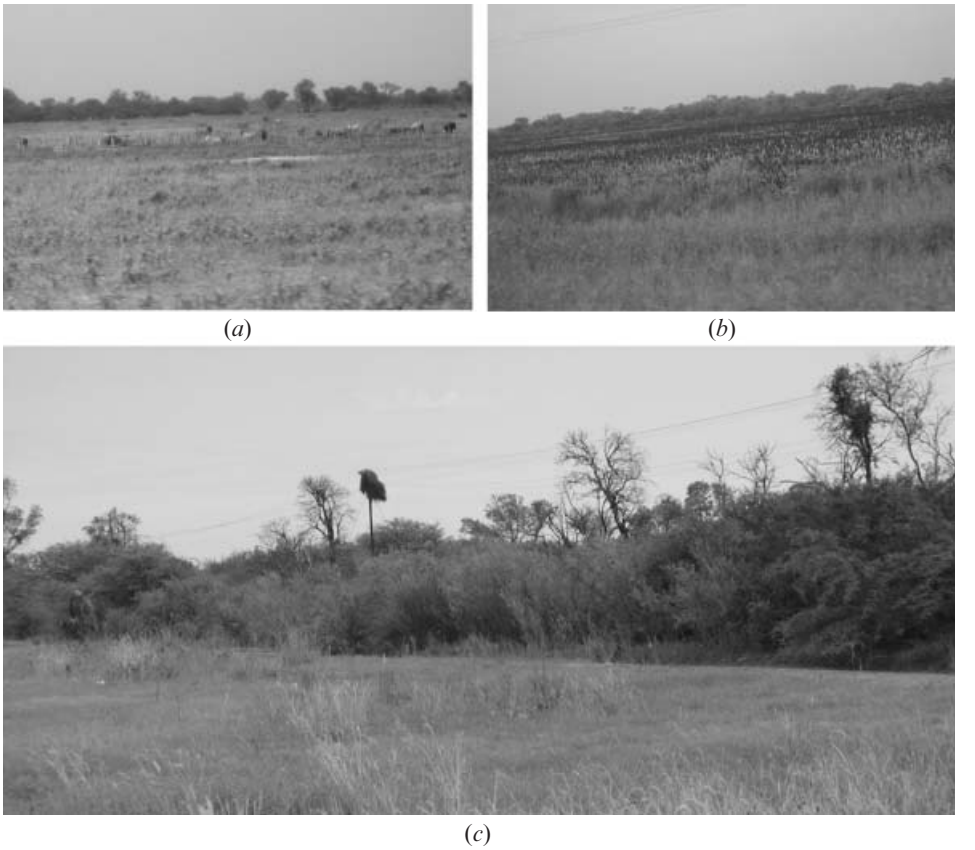

(*a*) (*b*)

(*c*)

Figure 4. Grassland area. (*a*) Grassland limited by strips of forest. (*b*) Sorghum, the dominant crop. (*c*) Strips of exploited forest. Gral. Belgrano Department, Santiago del Estero Province, Argentina.

According to the size of the farming estates given by INDEC (1989) and to the pixel size of the AVHRR Global Area Coverage (GAC) data (5776 ha), a mixed pixel is unavoidable for irrigated crops and grasslands, whereas for the other classes unmixed pixels may dominate. For irrigated crops, where 69% of the area is distributed in farming estates smaller than 100 ha, no properties over 1000 ha are recorded. For grasslands, only 27% of the area has properties larger than 5000 ha, whereas 47% of it is occupied by properties between 1000 and 5000 ha. The probability of mixed pixels decreases for rainfed crops, where 55% of the area corresponds to properties larger than 5000 ha; therefore, a uniform management is expected. Mixed pixels are also reduced for the native forest where properties are larger than 5000 ha in 70% of the total area.

We can therefore expect mixed pixels for all observations of irrigated cropland. Brunsell and Gillies (2003) examined the scaling rules of terrestrial vegetation using AVHRR-NDVI 1.1-km data over spatial scales from 2000 to 256 000 m (i.e. including our 7600-m scale). They concluded that the vegetation signature is scale invariant and that the NDVI vegetation signal is clear enough to be observed in the case of mixed pixels. This indication is confirmed by the results of Fuller and Prince (1996), who used 10-pixel samples for detailed analyses for Southern Africa.

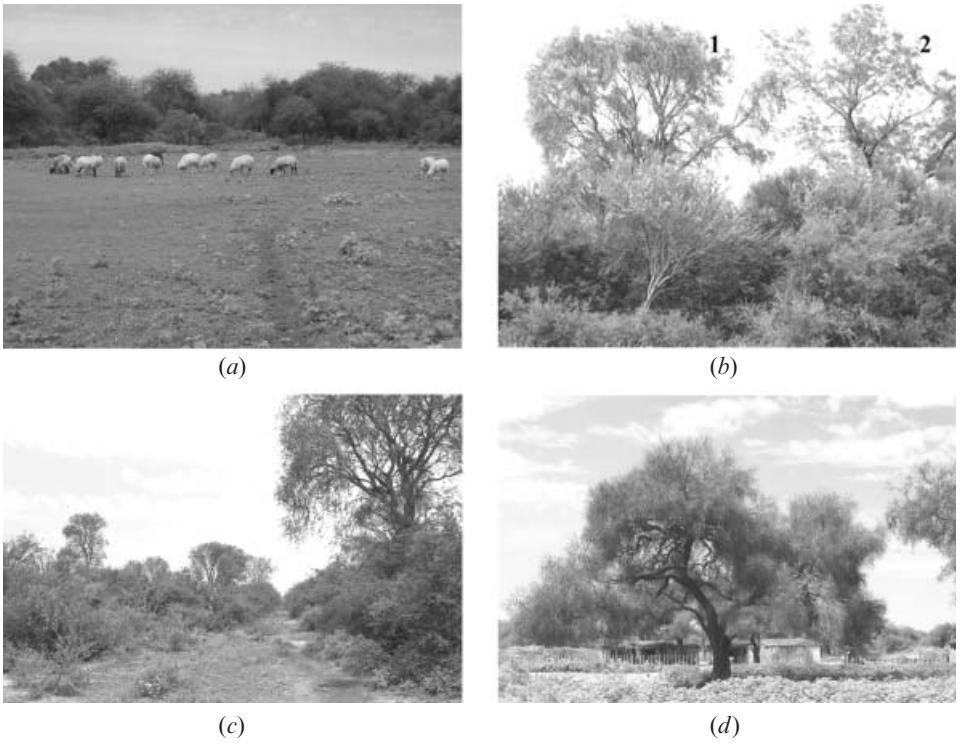

Figure 5. Native forest. (*a*) Patches of grassland around isolated settlements. (*b*) Main trees: 1, *Aspidosperma quebracho-blanco*; 2, *Schinopsis lorentzii.* (*c*) Forest crossed by a path showing two tree layers and high total cover. (*d*) Isolated settlement ('puesto') at Tintina with *Prosopis kuntzei* trees for shade and food. Moreno Department, Santiago del Estero Province, Argentina.

2.2 *Data used*

The original data comprised a set of monthly NOAA-/AVHRR NDVI GAC image data for South America, each image is a monthly composite of the maximum NDVI value for each pixel. Cloud detection was achieved by thresholding channel 5 temperatures, and cloud-contaminated pixels were eliminated by being assigned a zero value. The NDVI was then calculated for each date by keeping the maximum NDVI value for each pixel as a means to eliminate those pixels most affected by atmospheric contamination effects such as aerosols and water vapour. GAC data were obtained by the Global Inventory Monitoring and Modelling Systems (GIMMS) group at the NASA Goddard Space Flight Center from Local Area Coverage (LAC) data (1.1 km × 1.1 km) by averaging four pixels and skipping the fifth in the first line; the following two lines are skipped completely, and the fourth line was sampled and averaged like the first one. Finally, data were reprojected onto an equal-area projection and resampled by continent to create a database with a spatial resolution of 7.6 km × 7.6 km (Townshend 1992). Finally, a 9-year set of NDVI images, from July 1982 to June 1991 (108 images), was masked with the boundaries of Argentina and of every province to extract the study area of Santiago del Estero province, and to apply the FFT analyses on a per-pixel basis for the entire study area.

Monthly rainfall data were supplied by the Caldenius Foundation (Tucumán, Argentina) and the National Meteorological Service of Argentina (S.M.N.).

3. Methods

3.1 *Scheme of the methodological approach*

Available data were processed to determine rainfall anomalies and to perform the Fourier analysis separately. Our study approach involved three different aspects, described in the following subsections.

3.1.1 Rainfall anomalies. This analysis involved two steps:

- Detection of both positive and negative rainfall anomalies at a monthly level, taking into account subsequent monthly anomalies.
- Parameterization of rainfall anomalies and their temporal distribution using non-dimensional coefficients.

3.1.2 Fourier analysis. This analysis involved four steps:

- Calculation of the Fourier parameters for each separate yearly growing season over the 9 years spanned by observations by applying an FFT algorithm.
- Making a test of homogeneity and comparison of means of Fourier parameters for each 12-month period to establish whether there were any significant differences between growing seasons.
- Calculation of the contribution of the amplitude of each periodic component to the total amplitude variance for each growing season.
- Parameterization of the contribution of each periodic component to the total amplitude variance using non-dimensional coefficients.

3.1.3 Relationship between rainfall anomalies and Fourier parameters. This analysis involved three steps:

- Assessment of the association of Fourier parameters with negative rainfall anomalies for each 12-month period.
- Assessment of the contribution of each periodic component to the total amplitude variance in relation to rainfall anomalies.
- Evaluation of correlation of phenology (NDVI) and rainfall anomalies using non-dimensional coefficients.

3.2 *Rainfall anomalies*

3.2.1 Detection of drought events. We defined *drought* in this study, by analogy with the definition given by Bobba de González and Minetti (2001), as an event where rainfall was below the average of the study period (1982–91); we applied this definition to both monthly and yearly rainfall. We refer to positive rainfall anomalies, when rainfall is higher than the average over the period of interest, as *surplus*. Thus, negative (droughts) and positive rainfall (surplus) anomalies were calculated and recorded at monthly and yearly levels. As regards the four land cover types selected for this study, we considered a growing season (also called yearly growth cycle) as running from July (winter) to June (end of autumn) when rainfed crops are already harvested and natural vegetation and grasslands present low

biological activity. Rainfall anomalies and total yearly rainfall were evaluated accordingly; from July to June. In addition, we used the arithmetic sum of positive and negative anomalies as an indicator of rainfall variability throughout the year.

3.2.2 Parameterization of magnitude and temporal distribution of monthly rainfall anomalies. We used the following non-dimensional coefficients to represent concisely the magnitude and temporal distribution of rainfall anomalies:

Coefficient D: sum of negative anomalies
Coefficient S: sum of positive anomalies
Coefficient D/A: sum of negative anomalies/annual rainfall
Coefficient D/S: sum of negative anomalies/sum of positive anomalies
Coefficient DI/SI: duration of severe negative anomalies/duration of severe positive anomalies. This was calculated by multiplying the sum of negative, respectively positive, monthly anomalies greater than 10 mm by the number of consecutive months during which negative, respectively positive, anomalies occurred
Coefficient DI + SI: combined duration of severe negative and positive anomalies

3.3 *Fast Fourier Transform (FFT) analysis*

3.3.1 Calculation of Fourier parameters. In this study we used the Mixed Radix FFT algorithm developed by Verhoef (1996), Verhoef *et al.* (1996) and applied by Azzali and Menenti (1996).

This FFT algorithm was applied to the 108 monthly images of the study area organized in nine sets of 12-month NDVI images, each corresponding to a yearly growing season (July 1982 to June 1983, July 1983 to June 1984, etc.). Therefore, the FFT algorithm was run nine times, once for every growing season. As a result, a set of 12 images of Fourier parameters was obtained for each cycle: mean NDVI (frequency 0), amplitude and phase for the periods of 12 months (frequency 1), 6 months (frequency 2), 4 months (frequency 3), 3 months (frequency 4) and 2.4 months (frequency 5), and amplitude for the 2-month period (frequency 6). The results are expressed as digital numbers (DNs). Conversions between DNs and Fourier parameters are:

$$\text{Mean NDVI} : [(\text{DN} \times 4) - 511]/512 \text{ (ranging from } -1 \text{ to } +1)$$

$$\text{Amplitude} : (\text{DN}/2.5)/512 \text{ (ranging from 0 to 1)}$$

$$\text{12-month time lag in months} : [(\{[(\text{DN}/240) \times 360] - 180\}/180) \times 6] + 6, \text{ with}$$

the last two terms (6) being the semiperiod.

Therefore, the 6-month time lag in months is :

$$[(\{[(\text{DN}/240) \times 360] - 180\}/180) \times 3] + 3, \text{ and so on.}$$

Our analysis focused on the 12- and 6-month components because of the limited number of observations in the annual time series.

To assess the accuracy of the Fourier parameters estimated, the following test was performed. Image samples and cycles characterized by a contribution of the 12-month component to the total amplitude variance equal to 90%, or higher, were extracted from the available data. The yearly difference between minimum and

maximum NDVI was determined for each sample and cycle in the extracted subset of data, and a regression analysis against the amplitude of the 12-month component was performed. The high correlation obtained ($r=0.93$, $n=12$, $\alpha<0.001$) indicates that the estimates of the yearly amplitude obtained with the FFT algorithm were fairly accurate, despite the limited number of observations in each time series (i.e. 12-monthly values).

3.3.2 Sample homogeneity analysis. The homogeneity of the 10-pixel image samples used for our detailed analysis was assessed with the variance analysis ($\alpha=0.01$). The 10 contiguous pixels were selected for each land cover type within large patches to allow selection of pixels far from patch edges, even at the low spatial resolution of our AVHRR GAC data.

The homogeneity of each 10-pixel sample was analysed by taking the yearly Fourier parameters as the dependent variables (response variables) and the yearly growth cycles as the classification variable because they represent the source of variation (rainfall variability). This means that growth cycles allow yearly Fourier parameters (observations) to be separated into groups, as if they were describing the response of land cover under different treatments, for studying the effect of rainfall conditions of each growth cycle on yearly Fourier parameters (INFOSTAT 2002). The null hypothesis states that yearly Fourier parameters show no differences from one cycle to another. The alternative hypothesis states that there are differences in Fourier parameters from one cycle to another insofar as they characterize the phenology, and that these differences in phenology are explained by the major growth-controlling factor, rainfall (PP), that is:

$$H_0: FFT_{1982-83} = FFT_{1983-84\ldots} = FFT_{1990-91}$$
$$H_1: FFT_{1982-83} \neq FFT_{1983-84\ldots} \neq FFT_{1990-91}$$
$$\text{because } PP_{1982-83} \neq PP_{1983-84\ldots} \neq PP_{1990-91}$$

As each 10-pixel sample proved to be homogeneous, a comparison of means was carried out. For every cycle yearly Fourier parameters were compared by pairs using Fisher's least significant difference (LSD) test ($\alpha=0.01$). These statistical analyses were performed with InfoStat software (2002).

3.3.3 Amplitude variance. The variance of the amplitude of each periodic component was calculated to determine to what extent rainfall anomalies could modify the magnitude and time of occurrence of the yearly NDVI maximum. Variance was calculated according to Jakubauskas *et al.* (2001), who cited Davis (1986), where the variance of a time series is the sum of the variances of the individual terms.

The relative contribution of each periodic term to the total variance was calculated (for each pixel) by first computing the total variance as follows:

$$\text{Total variance} = \sum_{1}^{n} \left[\left(\text{amplitude}_j \right)^2 \Big/ 2 \right]$$

where j is each term (period) in the series and n is the total number of terms. The relative contribution of each term is computed by dividing the individual variance for each term by the total variance.

3.3.4 Parameterization of the contribution to amplitude variance using non-dimensional coefficients. A concise representation of vegetation phenology from

the full set of Fourier parameters was constructed by using the following non-dimensional coefficients:

Coefficient A: variance of the amplitude of the 6-month component/variance of the amplitude of the 12-month component
Coefficient B: sum of the variances of the amplitude of the 4- to 2-month components/variance of the amplitude of the 12-month component
Coefficient C: sum of the variances of the amplitude of the 6- to 2-month components/variance of the amplitude of the 12-month component

3.4 *Relationship between droughts and Fourier parameters*

3.4.1 Assessment of the association of yearly Fourier parameters with annual rainfall anomalies. Yearly Fourier parameters (mean NDVI, and amplitude and phase at the 12-month period) were analysed along with rainfall anomalies. Both were normalized to their corresponding averages over the period July 1982 to June 1991. The effect of drought on the Fourier parameters was contrasted with literature values, as a sort of ground truth, particularly for rainfed and irrigated crops.

3.4.2 Modification of contributions to amplitude variance due to drought. The largest and the smallest 12-month amplitude variance contributions were compared with all the other period contributions to determine to what extent the cycle pattern was modified by negative rainfall anomalies.

3.4.3 Correlations between coefficients of cycle structure and rainfall anomalies. The relationship between phenology and rainfall anomalies was also analysed by correlating the non-dimensional coefficients A, B and C with the non-dimensional coefficients D, D/A, D/S, DI/SI and DI + SI defined above. Correlations were calculated by using Pearson's ρ ($\alpha=0.05$) after verifying a normal distribution (Shapiro–Wilks test, $\alpha=0.05$); some variables were normalized by the natural logarithm.

4. Results and discussion

4.1 *Detection of drought events*

Monthly negative and positive anomalies and monthly NDVI presented different behaviour for each land cover type. A cycle rainfall budget, either positive (surplus) or negative (droughts), expressed the final results of the monthly rainfall anomalies (table 1).

Yearly droughts were not present in all meteorological stations for the same cycle; droughts were more frequent at the stations Santiago del Estero, Pozo Hondo and Tintina that have a hot semi-arid climate. Some droughts were coincident with climate events in Argentina, such as La Niña in 1984–85 and 1988–89 and El Niño in 1986–87 and 1987–88 (Seiler and Kogan 2002). The cycles 1988–89 and 1990–91 were in agreement with regional droughts detected by Bobba de González and Minetti (2001).

The distribution of monthly NDVI for irrigated crops shows a monomodal structure. Some positive rainfall anomalies were consistent with NDVI peaks; the clearest relationship with negatives anomalies was for the cycle 1988–89, where the monthly NDVI reached low values (figure 6).

For rainfed crops, the monthly NDVI shows a clear reaction to rainfall anomalies: for positive anomalies the NDVI response was clear in cycles 1983–84,

Table 1. Rainfall statistics for the meteorological stations associated with the selected land cover types: annual rainfall, sum of negative (droughts) and of positive (surplus) anomalies, annual balance of negative and positive anomalies (budget).

		Rainfall statistics (mm/year)								
Vegetation type		1982–83	1983–84	1984–85	1985–86	1986–87	1987–88	1988–89	1989–90	1990–91
Crops with irrigation	Rainfall	762	741	465	691	459	505	201	843	687
	Droughts	−70	−42	−153	−113	−208	−119	−402	−16	−156
	Surplus	235	161	27	197	73	56	0	255	266
	Budget	165	119	−126	84	−135	−63	−402	239	110
Rainfed crops	Rainfall	667	738	559	769	561	717	346	565	608
	Droughts	−18	−35	−190	−84	−126	−108	−330	−146	−40
	Surplus	100	174	147	214	63	223	53	92	55
	Budget	82	139	−43	130	−63	115	−277	−54	15
Grasslands	Rainfall	1042	1056	1232	977	897	695	836	1027	997
	Droughts	−149	−143	−23	−207	−272	−321	−273	−134	−242
	Surplus	265	213	339	184	112	100	91	208	233
	Budget	116	70	316	−23	−160	−221	−182	74	−9
Native forest	Rainfall	773	737	1064	711	1084	837	535	846	535
	Droughts	−196	−131	−86	−235	−121	−215	−255	−162	−308
	Surplus	197	66	375	138	371	276	0	227	55
	Budget	1	−65	289	−97	250	61	−255	65	−253

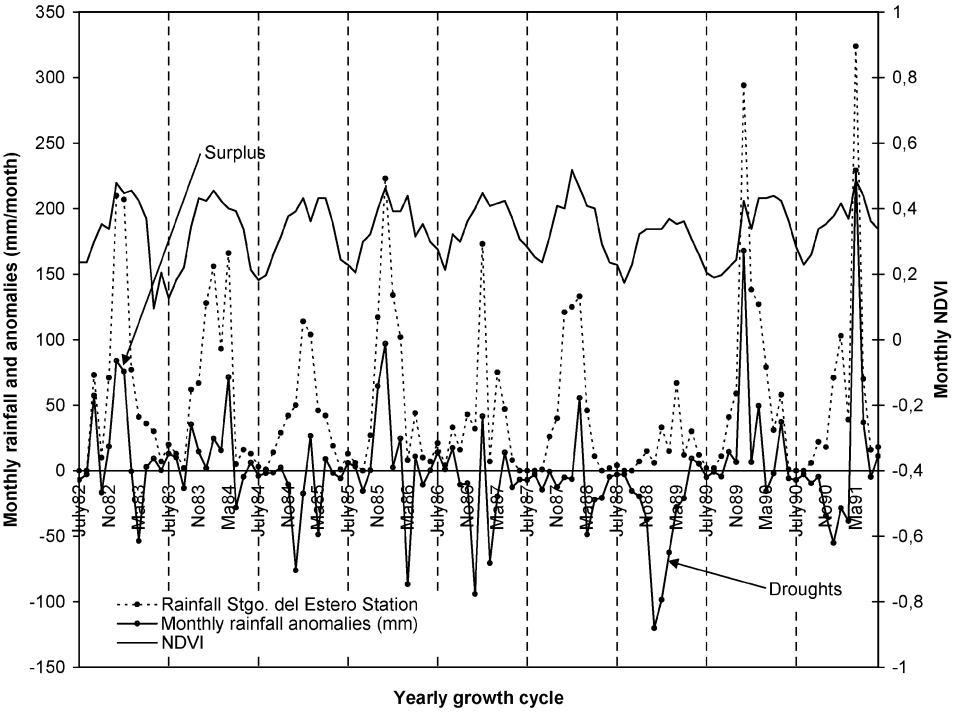

Figure 6. Irrigated crops: monthly rainfall, NDVI and rainfall anomalies (droughts and surplus) from the average for the period July 1982–June 1991.

1987–88, and for negative anomalies the cycles 1984–85, 1988–89 and 1989–90 show low NDVI values. There was a high contrast between the lowest and highest NDVI of each cycle in consonance with plowing activities and maximum greenness reached before harvesting (figure 7).

Grasslands show an irregular NDVI pattern, where there was some agreement with negative anomalies for cycles 1986–87 and 1988–89, and with positive anomalies in cycles 1984–85, 1985–86 and 1989–90. The contrast between the lowest and highest NDVI cycle values was not as high as for rainfed crops (figure 8).

The native forest shows a relatively uniform NDVI pattern with fast greening in spring despite some negative rainfall anomalies. This forest exhibited a limited response to extreme rainfall anomalies, such as the positive anomalies in 1984–85 and 1989–90 and the negative ones in 1985–86, 1988–89 and 1990–91 (figure 9).

4.2 *Detection of significantly different cycles*

The results of the variance analysis for the 10-pixel sample show that the differences in mean NDVI and 12-month amplitude and phase among the nine cycles were highly significant ($\alpha<0.001$) for all land cover classes. To establish whether the differences in yearly Fourier parameters were due to rainfall anomalies, a paired means test was performed (table 2). This test indicated that differences were significant ($\alpha=0.01$) in a large number of cases. The percentages of pairs of cycles (over the total number of combinations: 36) whose Fourier parameters were significantly different are summarized in table 3.

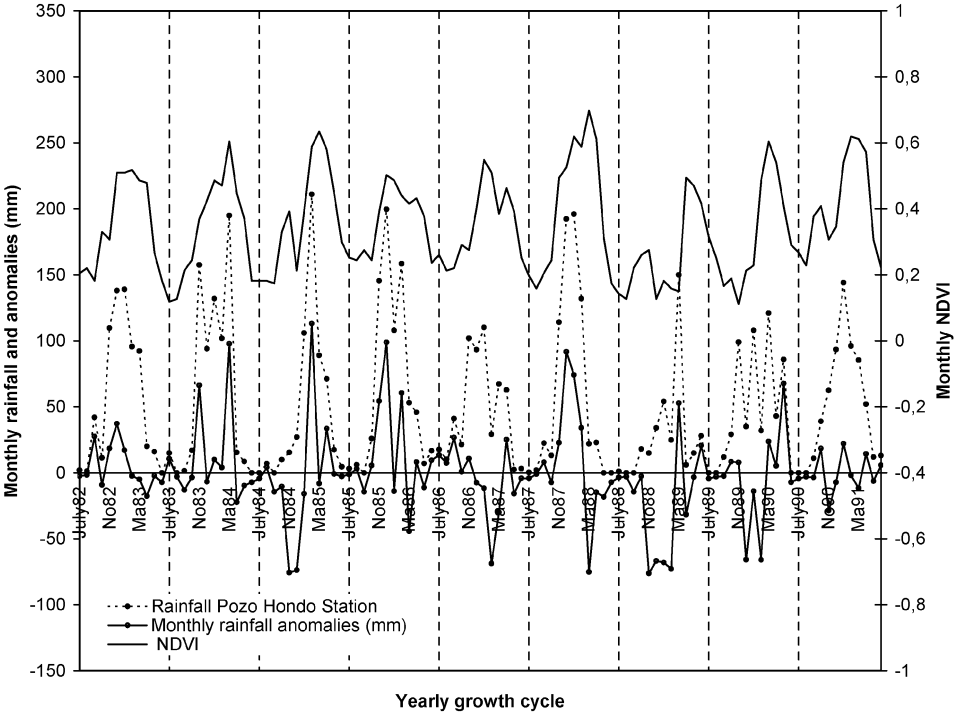

Figure 7. Rainfed crops: monthly rainfall, NDVI and rainfall anomalies (droughts and surplus) from the average for the period July 1982–June 1991.

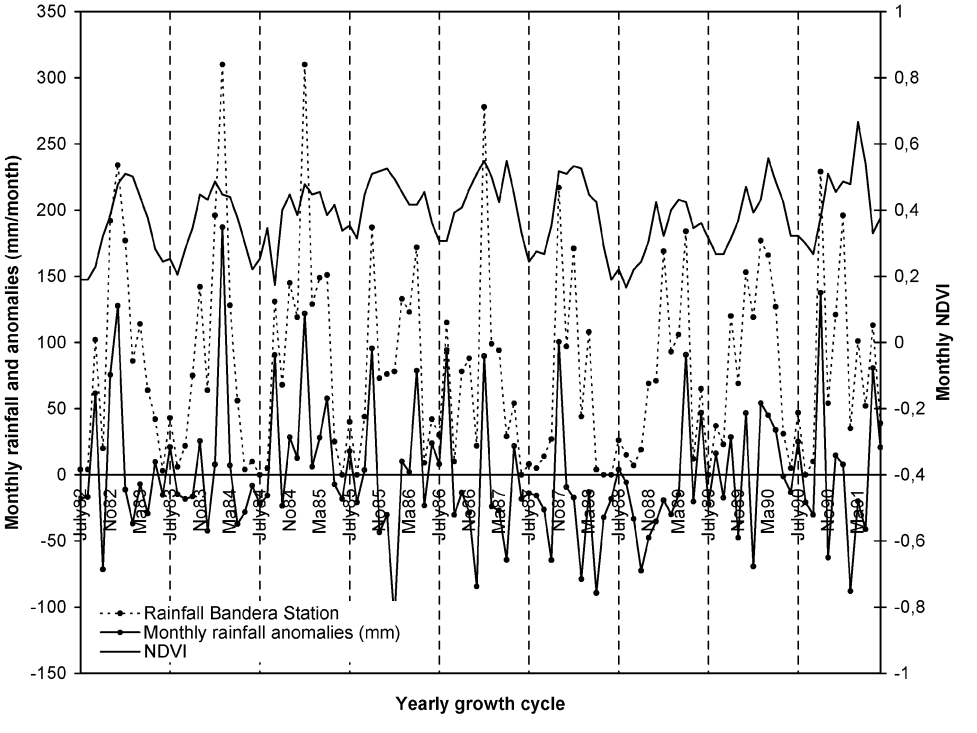

Figure 8. Grasslands: monthly rainfall, NDVI and rainfall anomalies (droughts and surplus) from the average for the period July 1982–June 1991.

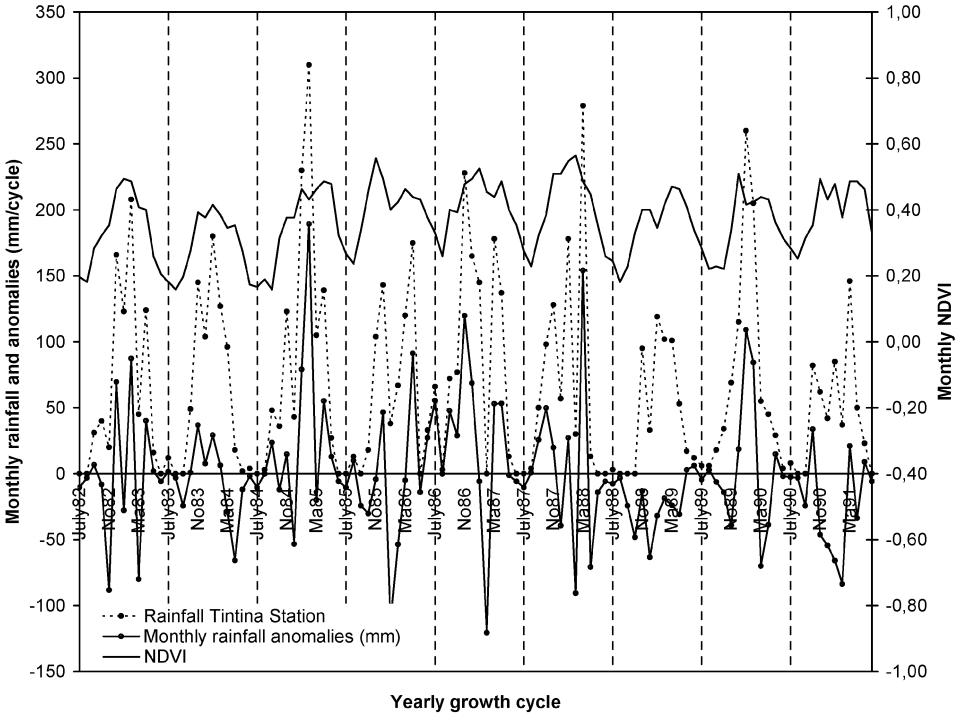

Figure 9. Native forest: monthly rainfall, NDVI and rainfall anomalies (droughts and surplus) from the average for the period July 1982–June 1991.

The native forest and grasslands show the largest number of pairs of significantly different cycles for mean NDVI (table 3). Irrigated and rainfed crops exhibited less interannual variability than native forest and grassland. With regard to amplitude, the native forest shows more irregular cycles than the other land cover classes; grasslands, however, presented the least interannual variability in yearly amplitude (table 3). Rainfed crops had more irregular cycles than did irrigated crops. Interannual variability in the time lag of maximum greenness was significant for grasslands and native forest and less significant for rainfed and irrigated crops.

Overall, interannual variability in yearly mean NDVI, amplitude and phase was larger for native forest and grasslands than for rainfed and irrigated crops. This indicates, as expected, a weaker response of agro-ecosystems to interannual variability in rainfall.

4.3 *Association of yearly Fourier parameters with annual rainfall anomalies*

The variation in mean NDVI, and amplitude and phase at the 12-month period, as well as rainfall, was normalized to the corresponding averages over the period 1982–91. The most relevant results are summarized in table 4.

4.3.1 Irrigated crops. Although crops were irrigated, the impact of scarcer rainfall was notable in 1984–85, 1986–87, 1987–88, and in the 1988–89 regional drought (table 1). When at least two continuous or isolated negative anomalies ($\geqslant$50 mm) occurred in summer (i.e. somewhere from December to February), the amplitude decreased as in the cycle 1986–87; this was also true for a cycle with a positive rainfall anomaly such as 1990–91, where continuous droughts occurred from

Table 2. Comparison of means between yearly cycles (LSD Fisher test, $\alpha=0.01$) for Fourier parameters and each land cover. Letters indicate a significant difference for mean NDVI (N), amplitude (A) and phase (P).

Irrigated crops

	1982–83	1983–84	1984–85	1985–86	1986–87	1987–88	1988–89	1989–90	1990–91	
1982–83			AP	AP	AP	AP	NAP	P	AP	1982–83
1983–84	A		AP	A	AP	NA	NAP	P	NAP	1983–84
1984–85	AP	NP					NA	P	AP	1984–85
1985–86	A	NA	AP				NA	NAP	P	1985–86
1986–87		NA	AP	A		A	NA	NAP	P	1986–87
1987–88	NA	NA	NAP	A	NA		NA	NP	AP	1987–88
1988–89	NAP	NAP	NAP	NP	NAP	NAP		NAP	NAP	1988–89
1989–90	P	P	NAP	NAP	AP	NAP	NAP		NA	1989–90
1990–91	NP	NA	NAP	A	N	AP	NAP	NP		1990–91
	1982–83	1983–84	1984–85	1985–86	1986–87	1987–88	1988–89	1989–90	1990–91	

Rainfed crops

Native forest

	1982–83	1983–84	1984–85	1985–86	1986–87	1987–88	1988–89	1989–90	1990–91	
1982–83		NA	NP	NAP	NA	N	NAP	NAP	NAP	1982–83
1983–84	A		NAP	NAP	NAP	NA	NAP	NP	NAP	1983–84
1984–85	NAP	NP		NAP	NAP	NP	NA	A	NAP	1984–85
1985–86	NAP	NAP	NAP		NAP	AP	NAP	NAP	NAP	1985–86
1986–87	NA	NA	NAP	P		NAP	NAP	NAP	NP	1986–87
1987–88	NP	NAP	AP	NAP	NAP		NAP	NAP	NAP	1987–88
1988–89	NAP	AP	NP	NP	NP	NAP			NAP	1988–89
1989–90	NAP	NP	P	NAP	NP	NAP	N		NAP	1989–90
1990–91	NA	NA	N	NP	N	AP	NP	NP		1990–91
	1982–83	1983–84	1984–85	1985–86	1986–87	1987–88	1988–89	1989–90	1990–91	

Grassland

N, NDVI; A, amplitude; P, phase.

Table 3. Percentage of pairs of cycles, over a total of 36 pairs, whose Fourier parameters are significantly different as the result of the comparison of means between cycles (LSD Fisher test, $\alpha=0.01$).

	Irrigated crops	Rainfed crops	Grassland	Native forest
NDVI	39	64	83	92
Amplitude	67	78	58	83
Phase	61	64	78	80

September to February (figure 7). When negative anomalies occurred only once (isolated) in summer or in spring and/or autumn, the amplitude increased when there was a recovery of NDVI after the anomaly. When monthly droughts were less than 50 mm in a month, irrigation was effective.

These tendencies were accentuated during the severe regional drought of 1988–89 (La Niña phase), where the 66% reduction in rainfall (i.e. as little as 201 mm) created temporarily arid conditions and a high dependence on irrigation. The mean NDVI was reduced by 3%, but the amplitude was reduced by 44%. This was a very different growth cycle; the mean NDVI and amplitude presented significant differences from the other eight cycles (table 2). Rainfall anomalies were continuous for nine months (August to April), that is the full growing season. In early spring (October), water for irrigation was still available and monthly NDVI values were normal, but then there were restrictions because the level of the Río Hondo dam became critical (Boletta *et al.* 1989). In the upper catchment area the river flow was reduced by 50% (EVARSA 2000) in accordance with droughts in the intermountain valleys, piedmont and plain (Trauth *et al.* 2000, Bobba de González and Minetti 2001). During this drought, air saturation deficit, wind speed and temperature were higher than the historical average (Boletta *et al.* 1989).

The limited interannual fluctuations of mean NDVI, 1–3% around the average, for the period 1982–91, when only 39% of paired cycles were significantly different (table 3), seemed to be explained by irrigation supply.

The Fourier parameters reacted not only to negative but also to positive rainfall anomalies. When the monthly rainfall surplus was in the summer and <250 mm, there was an increase in amplitude and a decrease in phase (cycles 1982–83 and 1983–84). When the monthly rainfall surplus was $\geqslant 250$ mm, not only did the amplitude increase but the phase also increased because of the longer growing season and greater time lag, to the point that the phase in cycle 1989–90 was significantly different from that of all the other cycles (table 2).

In conclusion, monthly rainfall anomalies have a significant impact on yearly Fourier parameters: the 12–month amplitude was the most sensitive parameter, and mean NDVI the least sensitive.

4.3.2 Rainfed crops. In the study area soya bean is sown between November and January, depending on the rainfall, and it takes 30–50 days to fully cover the soil (Fadda 1986). The harvest period extends mainly from the second half of April to the end of June, with most work concentrated in May (Ricci and Ploper 1989). The most drought-sensitive stage is full pod development in March. Four cycles with droughts were detected (1984–85, 1986–87, 1988–89 and 1989–90). Amplitude was the most frequently significantly different Fourier parameter from one cycle to another (tables 2 and 3).

When negative rainfall anomalies occurred in mid-summer (1986–87, 1990–91), the 12-month amplitude decreased. When there were adequate rains in mid-summer,

Table 4. Summary of main results on the relationship between Fourier parameters and rainfall anomalies (droughts and surplus) for the period July 1982–June 1991, for each land cover type.

Land cover/cycle	Irrigated crops	Rainfed crops	Grassland	Forest
1982–83	*Surplus of rainfall*: amplitude increased 24%, phase reduced 14%		*Adequate rainfall with previous dry cycle*: amplitude increased 35%	
1983–84	*Surplus of rainfall*: amplitude increased 32%, phase reduced 6%	*Adequate rainfall in spring–summer*: amplitude increased 19%, phase reduced 8%		
1984–85		*Droughts in spring–summer but adequate rainfall during critical soya bean period*: amplitude increased 10%	*Humid cycle*: amplitude reduced 26%	*Very humid cycle preceded by a dry autumn–winter*: amplitude increased 28%, phase increased 11%
1985–86	*Surplus of rainfall*: amplitude reduced 12%, phase reduced 6%	*Excesive rainfall in spring–summer*: amplitude reduced 27%, phase reduced 11%	*Humid cycle*: amplitude reduced 39%, phase reduced 20%	*Semi-arid cycle preceded by a very humid cycle, wet current autumn*: amplitude reduced 26%, phase reduced 9%
1986–87	*Droughts in spring and summer*: amplitude reduced 20%	*Drought during critical soya bean period*: amplitude reduced 17%, phase reduced 5%	*Dry spring preceded by a humid autumn*: amplitude reduced 12%	*Very humid cycle preceded by a humid autumn–winter*: amplitude reduced 26%, phase reduced 6%
1987–88		*Adequate rainfall in spring–summer*: amplitude increased 51%, phase reduced 10%, mean NDVI increased 4%	*Abondant rainfall in early summer but droughts in late summer*: amplitude increased 42%, phase reduced 9%	*Humid cycle preceded by very humid cycle, current dry autumn*: amplitude increased 34%, phase reduced 7%
1988–89	*Severe regional drought*: 50% reduction of rivers yield affecting irrigation, amplitude reduced 44%	*Severe regional drought with very late rainfall*: amplitude reduced 45%, phase increased 34%, mean NDVI decreased 7%	*Regional drought*: amplitude reduced 12%, phase increased 15%, mean NDVI reduced 4%	*Regional drought*: amplitude reduced 13%, phase increased 11%
1989–90	*Surplus of rainfall*: amplitude increased 17%, phase increased 17%			
1990–91	*Droughts from spring to summer*: amplitude reduced 20%, phase increased 9%	*Droughts in mid-summer and in critical soya bean period*: amplitude reduced 8%, phase reduced 7%		*Continuous droughts in spring–summer*: amplitude reduced 26%, phase increased 4%

amplitude increased (1984–85). Mean NDVI fluctuated ± 1% around the average, except for the 7% reduction during the drought of 1988–89. The increase in mean NDVI was explained by rainfall surplus (1987–88).

For the drought of 1988–89, total rainfall fell by 44% (346 mm), reaching the level of Dry Chaco (300–500 mm/year; Casas 1994) and rains were concentrated in late summer. From September to February there was a deficiency of 279 mm (figure 7), causing late sorghum sowing, a dry-blooming period for soya bean in February, and irregular harvesting; autumn rainfalls were too late to reverse the damage caused by the lowest yield of the period 1982–91 (Bolsa de Cereales 1989). As a consequence, mean NDVI shows a reduction of 7% but amplitude decreased by 45% in agreement with the 44% rain reduction; phase, with an increase of 34%, expressed the important delay in maximum greenness that occurred in mid-autumn. Amplitude and phase parameters were more sensitive to low rainfall compared with mean NDVI.

4.3.3 Grasslands. Three contiguous cycles with droughts were detected: 1986–87, 1987–88 and 1988–89. From these cycles, the drought in 1987–88 was the most critical, with a 42% increment in amplitude due to the contrast between the high NDVI in response to rainfall surplus in early summer and the very low NDVI at the end of the cycle, consistent with monthly anomalies between February and May (table 1 and figure 8).

During the cycle 1988–89, continuous droughts occurred from spring to early summer, and as a consequence there was a reduction in the mean NDVI and amplitude and an increase in phase. The amplitude reduction was the result of very low maximal NDVI, after the lowest winter NDVI derived from the previous dry year. The increase in phase was due to vegetation recovery with the January rainfall, after a dry spring.

The cycle 1986–87 presented a dry spring during which grasslands with high cover from the previous humid autumn (1985–86) maintained good cover during the current growth cycle despite the continuous droughts from the end of summer to the start of autumn. As a consequence, there was an increase in mean NDVI and a reduction in amplitude.

The cycle 1982–83 showed a good and constant evolution of NDVI, giving a high contrast with the previous dry cycle that led to an increase in amplitude. The continuously humid years caused an amplitude reduction for the cycles 1984–85 and 1985–86.

For grasslands, when isolated anomalies in spring or summer (even greater than –50 mm) were followed by average or surplus rainfall, there was vegetation recovery (1982–83, 1986–87, 1990–91). After three or four contiguous negative anomalies in spring–summer (1985–86), a high rainfall surplus was necessary for recovery (figure 8).

The 12-month phase value decreased when maximum rainfall occurred in spring, and increased when rainfall surplus was in late summer–early autumn. The same was found for northeastern Brazil, where phase agreed within one month with the month of maximum rainfall (Negrón Juárez and Liu 2001).

4.3.4 Native forest. In contrast to herbaceous species, the forest responds to hydrological conditions over a period of time longer than a year. When the previous humid condition was combined with a rainfall surplus in spring and summer, both mean NDVI and 12-month amplitude increased, despite some anomalies in summer

(1987–88). This was also true for northeastern Brazil, where the lower amplitude and higher mean NDVI values indicated that the area had a wetter and longer rainy season (Negrón Juárez and Liu 2001).

A decrease in mean NDVI was generally associated with an increase in amplitude due to low rainfall in the spring (28% decrease in 1982–83 and 1984–85), producing a higher minimum–maximum contrast (figure 9). A decrease in amplitude was associated with a high NDVI in the previous autumn (1985–86, 1986–87, 1990–91) or with the opposite, a low vegetation development due to long periods of drought (1988–89).

The Fourier parameters seem to respond to both negative and positive monthly rainfall anomalies but not in an unequivocal way. Water availability in the previous cycle should be considered, particularly for natural vegetation, where weather conditions may make greening last longer and produce green biomass in winter, reducing the winter–summer contrast. Previous rainfall conditions were also important in the study by Malo and Nicholson (1990), who found that in western Sahel the correlation between woodland NDVI and rainfall increased when considering total rainfall over the 3 months preceding each NDVI observation.

4.4 *Amplitude variance and droughts*

The results summarized above indicate that the Fourier parameter most sensitive to rainfall anomalies was the 12-month amplitude. For the four land cover types considered above, the largest fraction (78–86%) of amplitude variance was explained by the 12-month amplitude. Two extreme cases, the highest and the lowest 12-month amplitude variance contribution, were analysed in more detail (figure 10).

For irrigated crops, the 12-month amplitude explained, on average, 86% (78.7–92.2%) of the total amplitude variance, followed by the 6-month period (6.5%) and the 3-month period (4.5%). The cycle 1989–90, with the least negative anomaly (–16 mm, coefficient D/S=0.06) and normal irrigation water supply, shows the 12-month amplitude accounting for 90% of the total variance. The remaining 10% was accounted for by the 6- and 4-month Fourier components. On the contrary, the cycle 1988–89 shows a 16% contribution of the 6-month amplitude to the total variance, clearly due to the total water deficit of 402 mm, where irrigation was not sufficient to offset the lower rainfall.

For rainfed crops, the 12-month period amplitude explained, on average, 78.2% (29.9–94.3%) of the total amplitude variance, followed by the 6-month (13.2%) and the 4-month Fourier component (4.2%). During the cycle 1982–83, rainfed crops were affected by small rainfall anomalies (−18 mm) (coefficient D/S=0.18), with a 93% contribution of the 12-month component to the total variance. For the cycle 1988–89, a severe negative anomaly of 330 mm resulted in a 53% contribution of the 6-month component and a 30% contribution of the 12-month component to the total variance.

For grasslands, the 12-month period explained, on average, 83.2% (62–99.7%) of the total amplitude variance, followed by the 6-month period (5.3%) and the 4-month period (4.6%). Grasslands comprise both annual and perennial species, and humid conditions produced different peaks in the NDVI time series. Grasslands show for the cycle 1982–83 a 'perfect' monomodal cycle, where the 12-month amplitude contributed 99.7% of the total variance with isolated anomalies in spring and summer (−119 mm, coefficient D/S=0.56) (figure 8). The major change in the annual cycle structure was observed in 1984–85, when the contribution of the

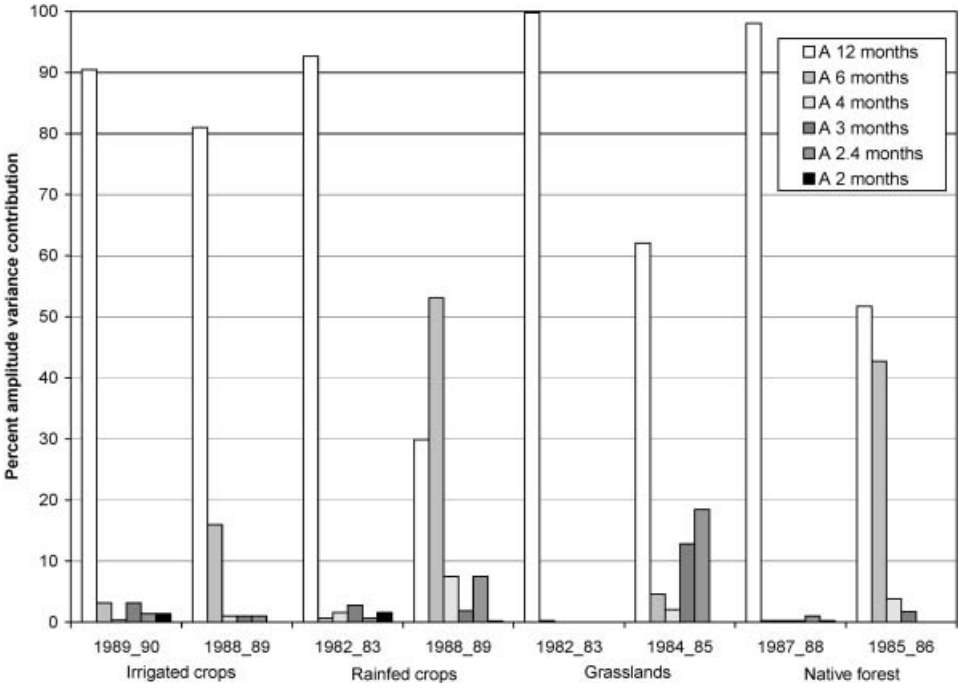

Figure 10. Amplitude variance contribution of each component to the total amplitude variance for irrigated and rainfed crops, grasslands and native forest. Two extreme cases of 12-month amplitude variance contribution for each land cover type are presented.

12-month component was reduced to 62% with almost no negative anomalies (−23 mm; coefficient D/S=0.07). In this case the 4- and 2-month components accounted for 33% of the total variance, explained by the 339 mm rainfall surplus from September to May, with an annual rainfall of 1232 mm (table 1).

For the native forest, the 12-month component accounted, on average, for 81.4% (51.7–98%) of the total amplitude variance, followed by the 6-month component (13.2%). During the cycle 1987–88, the 12-month component contributed 98% of the total variance. This 'almost perfect' monomodal structure was explained by the important rains that followed isolated anomalies during the summer (−130 mm, coefficient D/S=0.78) and allowed a good vegetation recovery. By contrast, during the cycle 1985–86, the 12-month component accounted for 52% of the total variance, whereas the contribution of the 6-month component increased to 43% because of two continuous anomalies in spring (−54 mm) and summer (−167 mm, coefficient D/S=1.71) (figures 9 and 10).

4.5 *Correlations between the annual NDVI temporal profile and rainfall anomalies*

To evaluate the correlation of the NDVI temporal profile with magnitude and temporal distribution of rainfall anomalies, we defined the appropriate indicators (see section 3). The correlation was significant (α=0.05) for irrigated and rainfed crops (table 5). For both crops the positive correlation with total rainfall anomaly (i.e. droughts) (coefficient D) shows that as the annual rainfall deficit increased, the contribution of the shorter-period components increased as well. The occurrence of positive rainfall anomalies did not modify this trend: the shorter-period components

Table 5. Irrigated and rainfed crops correlations between coefficients of rainfall anomalies and coefficients of cycle structure (ρ Pearson, $\alpha=0.05$).

	Coefficients of cycle structure anomalies by means of Fourier amplitude at different periods			
		Rainfed crops		
Coefficients of rainfall anomalies	Irrigated crops Coefficient A	Coefficient A*	Coefficient B*	Coefficient C*
Coefficient D	$r=0.68$ $p=0.04$	NC	$r=0.77$ $p=0.01$	$r=0.80$ $p=0.01$
Coefficient D/A*	NC	NC	$r=0.72$ $p=0.03$	$r=0.75$ $p=0.02$
Coefficient D/S*	$r=0.71$ $p=0.03$	$r=0.69$ $p=0.04$	$r=0.78$ $p=0.01$	$r=0.84$ $p=0.004$
Coefficient DI/SI*	NC	$r=0.69$ $p=0.04$	NC	$r=0.77$ $p=0.02$
Coefficient DI+SI	NC	$r=-0.76$ $p=0.02$	NC	$r=-0.81$ $p=0.01$

NC, no significant correlation.
*Variables normalized by applying natural logarithm.

were significant when negative anomalies were larger than positive ones (coefficients D/S and DI+SI).

Despite the previously discussed association of the 12-month Fourier parameters with negative anomalies, no significant correlation was observed for grasslands or native forest. No present correlations between any coefficient of cycle anomaly and any coefficient of rainfall anomalies can be explained because this might be due to the humid conditions during the previous cycle, which is not taken into account by our analyses of separate yearly segments of the entire time series. Moreover, rainfed crops are shallow-rooted, whereas perennial grasslands, shrubs and trees explore deeper soil depths with their rooting system, thereby having access to a larger soil water reservoir.

With regard to irrigated crops, a significant correlation was observed between the magnitude of the 6-month component (coefficient A) and the magnitude of negative rainfall anomalies (coefficients D and D/S). For rainfed crops, the correlation observed was between the magnitude of components with a period shorter than 6 months (coefficient B) and total rainfall deficit (coefficients D and D/A). Correlation improved slightly when also considering the 6-month component (coefficient C). The 6-month component (coefficient A) was important when looking at correlations with positive rainfall anomalies. The duration of both positive and negative rainfall anomalies (coefficients DI/SI and DI+SI) was relevant for the 6-month component. Overall, the highest correlations were observed when taking into account all the periodic components (coefficient C).

5. Conclusions

The time series of monthly NOAA-AVHRR NDVI GAC data, although at coarse spatial resolution, provides a useful set of data to detect vegetation changes through the yearly growth cycle. The Fourier parameters determined with the FFT algorithm were useful for characterizing each yearly growth cycle. Significant interannual variability in their values was observed in response to water availability, that is both negative and positive rainfall anomalies. The Fourier parameters provided a particularly sensitive indicator of droughts.

The impact of rainfall anomalies on vegetation phenology was revealed by changes in the values of mean NDVI, amplitude and phase of the 12-month component. These Fourier parameters were not equally sensitive to rainfall anomalies: the 12-month amplitude was the most sensitive and mean NDVI the least sensitive. The impact of rainfall anomalies on the Fourier parameters was related to vegetation type and to the phenological stage at the time of occurrence of the anomaly. The Fourier parameters were most sensitive to rainfall anomalies in the case of rainfed crops. Interannual variability in the phase value was explained by the time of occurrence of the negative anomalies and the eventual recovery due to rainfall later in the growing season.

The amplitude of the 12-month component decreased for irrigated crops when at least two continuous or isolated important negative anomalies occurred in summer, and increased in the case of positive rainfall anomalies. Mid-summer soil moisture conditions were critical for rainfed crops: a significant decrease was observed in the case of negative anomalies and a significant increase in that of positive anomalies. For permanent grasslands and forest, greenness at the end of the previous cycle had an important influence on the 12-month amplitude and also on the mean NDVI.

The Fourier parameters provided a very sensitive indicator of droughts in land cover types with monomodal growth cycles. Their sensitivity was shown by changes in the contribution of the 12-month component to the total amplitude variance, with an increase in the contribution of components with a period of 6 months or less. Negative rainfall anomalies modified the monomodal cycle structure of the annual NDVI temporal profile typical of rainfed and irrigated crops. The contribution of the 6-month component to the total amplitude variance also increased for the native forest in the case of negative anomalies. For grasslands, under a humid climate, positive rainfall anomalies were determinant of changes in the monomodal structure of the annual NDVI temporal profile, thereby increasing the contribution of the 4- to 2-month components.

Concerning correlations between coefficients of cycle structure and rainfall anomalies, only irrigated and rainfed crops show correlations. For both crops the positive correlation with droughts shows that as annual rainfall deficit increased, so did the contribution of the shorter-period components. The highest correlation was observed for rainfed crops, as rain is the only water source and these crops have a shallow rooting system. For grasslands and forest, the high dependence of amplitude on the humidity conditions of the previous autumn and the multilayered vegetation canopy of deciduous and perennial species of the native forest that explore different soil layers may explain the absence of correlation between the structure of the NDVI temporal profile and rainfall anomalies.

Acknowledgements

The senior author wishes to remember Prof. María Elina González Loyarte de Roccasalva, her beloved elder sister. The authors are grateful to the anonymous referees for their comments and suggestions, which greatly improved the manuscript and generated further analysis. Thanks also to their Dutch colleagues G. Roerink, S. Azzali, C. Jacobs, M. Boss and H. Pelgrum for their scientific support and friendship during the stay at the Winand Staring Centre – DLO, Wageningen. M. M. González Loyarte thanks N. Horak for her valuable assistance with the English text, and M. C. Scoones and G. S. Farías (MAGRAF-CRICYT/CONICET) for the preparation of most of the figures. Support during field work in Santiago del Estero

by L. De Zordo, P. Araujo, M. Iturre, V. Mariot and J. Ledesma is gratefully acknowledged. The rainfall data used in this study were kindly provided by the Caldenius Foundation (Tucumán, Argentina) and the National Meteorological Service (S.M.N.). This research project was funded by the European Community and the National Council for Scientific and Technical Research of Argentina (PEI 0326/99).

References

ANYAMBA, A. and TUCKER, C.J., 2005, Analysis of Sahelian vegetation dynamics using NOAA-AVHRR NDVI data from 1981–2003. *Journal of Arid Environments*, **63**, pp. 596–614.

AZZALI, S., and MENENTI, M. (Eds), 1996, *Fourier Analysis of Temporal NDVI in the Southern African and American Continents* (Wageningen, the Netherlands: Winand Staring Centre for Integrated Land, Soil and Water Research).

AZZALI, S. and MENENTI, M., 2000, Mapping vegetation–soil–climate complexes in southern Africa using temporal Fourier analysis of NOAA-AVHRR data. *International Journal of Remote Sensing*, **21**, pp. 973–996.

BIANCHI, A.R. and YAÑEZ, C.E., 1992, *Las precipitaciones en el noroeste argentino (Rainfall in northwestern Argentina)* (Salta: INTA, EEA Salta).

BOBBA DE GONZÁLEZ M.E. and MINETTI, J.L., 2001, Las sequías en la región del NOA por áreas morfológicas (Droughts in the northwestern region of Argentina (NOA) by morphological area). *Revista del Departamento Geografía*, **6**, pp. 3–15 (Tucumán, Argentina: Universidad Nacional de Tucumán).

BOLETTA, P.E., ACUÑA, L.R. and JUAREZ DE MOYA M.L., 1989, *Análisis de las características de la Provincia de Santiago del Estero y comportamiento del tiempo durante la sequía de la campaña agrícola 1988/89 (Analysis of the characteristics of Santiago del Estero province and weather behaviour during the drought in the agricultural season 1988/89)* (Santiago del Estero, Argentina: INTA-UNSE).

BOLSA DE CEREALES, 1989, *Número Estadístico 1989 (Statistics Issue 1989)* (Buenos Aires, Argentina: Bolsa de Cereales).

BRUNIARD, E.D., 1982, La diagonal árida argentina: un límite climático real (The Argentinian arid diagonal: a real climatic boundary). *Revista Geográfica Intituto Panamericano de Geografía e Historia*, **95**, pp. 5–20.

BRUNSELL, N.A. and GILLIES, R.R., 2003, Determination of scaling characteristics of AVHRR data with wavelets: application to SGP97. *International Journal of Remote Sensing*, **24**, pp. 2945–2957.

CASAS, R.R., 1994, La disyuntiva del Chaco Occidental (The dilemma of the Western Chaco). *INTA Campo y Tecnología*, **3**, pp. 55–56.

DAVIS, J.C., 1986, *Statistics and Data Analysis in Geology* (New York: Wiley).

EVARSA, 2000, *Estadística Hidrológica Año 2000 (Hydrological Statistics Year 2000)* (Buenos Aires, Argentina: Subsecretaría de Recursos Hídricos, Evaluación de Recursos S.A.).

FADDA, G.S., 1986, Los suelos y su manejo en el área sojera del NOA (Soils and their management in the soya bean area in northwestern Argentina (NOA)). *Revista de la Asociación Argentina de la Soja*, **6**, pp. 14–17.

FULLER, D.O. and PRINCE, S.D., 1996, Regional-scale foliar phenology in tropical Southern Africa: an application of the Fast Fourier Transform to time series of satellite imagery. In *Fourier Analysis of Temporal NDVI in the Southern African and American Continents*, S. Azzali and M. Menenti (Eds), pp. 113–132 (Wageningen, the Netherlands: Winand Staring Centre for Integrated Land, Soil and Water Research).

GONZÁLEZ LOYARTE, M.M., 1995, La diagonale aride argentine: une realité écologique oscillante (The Argentinian arid diagonal: a shifting ecological reality). *Sécheresse*, **6**, pp. 35–44.

González Loyarte, M.M., 1996, Study of the variability of vegetation cover in Argentina. In *Fourier Analysis of Temporal NDVI in the Southern African and American Continents*, S. Azzali and M. Menenti (Eds), pp. 83–112 (Wageningen, the Netherlands: Winand Staring Centre for Integrated Land, Soil and Water Research).

González Loyarte, M.M. and Menenti, M., 2000, Usefulness of Fourier parameters to detect regional and local droughts within a time series of NOAA/AVHRR-NDVI data (GAC). In *Time Series of Satellite Data: Development of New Products*, G.J. Roerink and M. Menenti (Eds), pp. 63–70 (Wageningen, the Netherlands: Netherlands Remote Sensing Board).

Gurgel, H.C. and Ferreira, N.J., 2003, Annual and interannual variability of NDVI in Brazil and its connections with climate. *International Journal of Remote Sensing*, **24**, pp. 3595–3609.

Henricksen, B.L., 1986, Reflections on drought: Ethiopia 1983–1984. *International Journal of Remote Sensing*, **7**, pp. 1447–1451.

Henricksen, B.L. and Durkin, J.W., 1986, Growing period and drought early warning in Africa using satellite data. *International Journal of Remote Sensing*, **7**, pp. 1583–1608.

Hielkema, J.U., Prince, S.D. and Astle, W.L., 1986, Rainfall and vegetation monitoring in the Savanna Zone of the Democratic Republic of Sudan using the NOAA Advanced Very High Resolution Radiometer. *International Journal of Remote Sensing*, **7**, pp. 1499–1513.

Hoffmann, J.A., 1988, Las variaciones climáticas ocurridas en la Argentina desde fines del siglo pasado hasta el presente (Climate variations occurred in Argentina from the end of last century to the present). In *El deterioro del ambiente en la Argentina*, PROSA-FECIC (Ed.), pp. 275–290 (Buenos Aires: PROSA-FECIC).

Hueck, K., 1978, *Los Bosques de Sudamérica. Ecología, composición e importancia económica (South American forests. Ecology, composition and economic importance)* (Eschborn, Germany: German Association for Technical Cooperation (GTZ)).

INDEC, 1989, Censo Nacional Agropecuario 1988. Resultados Generales. Provincia de Santiago del Estero (National agricultural census of 1988. General Results. Santiago del Estero Province). *Censo Nacional Agropecuario de 1988*, **25**, pp. 1–50 (Buenos Aires: Instituto Nacional de Estadísticas y Censos).

INFOSTAT, 2002, *InfoStat Versión 1.1. Manual del Usuario (InfoStat Version 1.1. User's Manual)* (Córdoba, Argentina: Editorial Brujas).

Jakubauskas, M.E., Legates, D.R. and Kastens, J.H., 2001, Harmonic analysis of time-series AVHRR NDVI data. *Photogrammetric Engineering and Remote Sensing*, **67**, pp. 461–470.

Justice, C.O., Dugdale, G., Townshend, J.R.G., Narracott, A.S. and Kumar, M., 1991, Synergism between NOAA-AVHRR and Meteosat data for studying vegetation development in semi-arid West Africa. *International Journal of Remote Sensing*, **12**, pp. 1349–1368.

Justice, C.O., Holben, B.N. and Gwynne, M.D., 1986, Monitoring East African vegetation using AVHRR data. *International Journal of Remote Sensing*, **7**, pp. 1453–1474.

Justice, C.O., Townshend, J.R.G., Holben, B.N. and Tucker, C.J., 1985, Analysis of the phenology of global vegetation using meteorological satellite data. *International Journal of Remote Sensing*, **6**, pp. 1271–1318.

Ledesma, R.N. and Ledesma, F.A., 1983, La degradación del ecosistema en el Chaco seco (The degradation of the Dry Chaco ecosystem). *IDIA Instituto Nacional de Tecnología Agropecuaria*, **417–420**, pp. 71–79.

Le Houérou, H.N., 1999, *Estudios e investigaciones ecológicas de las zonas áridas y semiáridas de Argentina (Studies and ecological research on the arid and semiarid areas of Argentina)* (Mendoza, Argentina: Instituto Argentino de Investigaciones de las Zonas Áridas).

Liu, W.T. and Negrón Juárez, R.I., 2001, ENSO drought onset prediction in northeast Brazil using NDVI. *International Journal of Remote Sensing*, **22**, pp. 3483–3501.

MALO, A.R. and NICHOLSON, S.E., 1990, A study of rainfall and vegetation dynamics in the African Sahel using normalized difference vegetation index. *Journal of Arid Environments*, **19**, pp. 1–24.

MENENTI, M., AZZALI, S., VERHOEF, W. and VAN SWOL, R., 1991, *Mapping Agroecological Zones and Time Lag in Vegetation Growth by Means of Fourier Analysis of Time Series of NDVI Images. Monitoring Agroecological Resources with Remote Sensing and Simulation (MARS)* (Wageningen, the Netherlands: Winand Staring Centre for Integrated Land, Soil and Water Research).

MENENTI, M., AZZALI, S., DE VRIES, A., FULLER, D. and PRINCE, S., 1993, Vegetation monitoring in southern Africa using temporal Fourier analysis of AVHRR/NDVI observations. In *Proceedings of International Symposium on Remote Sensing in Arid and Semi-arid Regions, Lanzhou, China*, 1993 (Lanzhou, China: Chinese Academy of Science), pp. 287–294.

MINETTI, J.L. and SIERRA, E.M., 1984, La expansión de la frontera agrícola en Tucumán y el diagnóstico climático (Expansion of the agricultural boundary in Tucumán and climate diagnosis). *Rev. Ind. y Agrícola de Tucumán – RIAT*, **61**, pp. 109–126.

MINETTI, J.L. and ACUÑA, L.R., 1997, *Ocho décadas de precipitaciones promedio en la Provincia de Santiago del Estero. Período 1911–1990 (Eight decades of average rainfall in Santiago del Estero Province. Period 1911–1990)* (Santiago del Estero: INTA-EEA Sgo. del Estero and Tucumán: Fundación Caldenius).

MINETTI, J.L. and BOBBA DE GONZÁLEZ M.E., 1998, Las sequías regionales en el Noroeste Argentino (Regional droughts in Northwestern Argentina). *Revista del Departamento Geografía*, **4**, pp. 43–49 (Tucumán, Argentina: Universidad Nacional de Tucumán).

MOODY, A. and JOHNSON, D.M., 2001, Land-surface phenologies from AVHRR using the discrete Fourier transform. *Remote Sensing of Environment*, **75**, pp. 305–323.

NEGRÓN JUÁREZ, R.I. and LIU, W.T., 2001, FFT analysis on NDVI annual cycle and climatic regionality in Northeast Brazil. *International Journal of Climatology*, **21**, pp. 1803–1820.

POBLETE, A.G., MINETTI, J.L. and SIERRA, E.M., 1989, La influencia del régimen hídrico andino puneño en el oasis del Noroeste Argentino y Cuyo (Influence of the Andean Puna water regime on the oases of Northwestern Argentina and the Cuyo region). *Revista de Geofísica IPGH- Instituto Panamericano de Geografía e Historia*, **30**, pp. 137–149.

POTTER, C.S. and BROOKS, V., 1998, Global analysis of empirical relations between annual climate and seasonality of NDVI. *International Journal of Remote Sensing*, **19**, pp. 2921–2948.

POVEDA, G. and SALAZAR, L.F., 2004, Annual and interannual (ENSO) variability of spatial scaling properties of a vegetation index (NDVI) in Amazonia. *Remote Sensing of Environment*, **93**, pp. 391–401.

RICCI, O.R. and PLOPER, L.D., 1989, El cultivo de la soja en la Subregión Noroccidental (Soya bean cultivation in the Northwestern Subregion). *Revista de la Asociación Argentina de la Soja*, **9**, pp. 45–56.

ROERINK, G.J., MENENTI, M., SOEPBOER, W. and Z., S.U., 2003, Assessment of climate impact on vegetation dynamics by using remote sensing. *Physics and Chemistry of the Earth, Parts A/B/C*, **28**, pp. 103–109.

ROIG, F.A., ABRAHAM, E.M., DALMASSO, A., GONZÁLEZ LOYARTE, M.M., MARTÍNEZ CARRETERO, E., MÉNDEZ, E. and ROIG, V.G., 1988, *Documento de base para un plan nacional de acción para combatir la desertificación en la República Argentina (Basic document for a national plan of action to combat desertification in Argentina)* (Mendoza, Argentina: Instituto Argentino de Investigaciones de las Zonas Aridas-UNEP).

SEILER, R.A. and KOGAN, F., 2002, Monitoring ENSO cycles and their impacts on crops in Argentina from NOAA-AVHRR satellite data. *Advances in Space Research*, **30**, pp. 2489–2493.

TORRES BRUCHMANN, E., 1981, *Climatología general y agrícola de la Provincia de Santiago del Estero (General and agricultural climatology of Santiago del Estero Province)* (Tucumán, Argentina: U. N. de Tucumán).

TOWNSHEND, J.R.G. (Ed.), 1992, *Improved Global Data for Land Applications: A Proposal for a New High Resolution Data Set* (Stockholm, Sweden: International Geosphere Biosphere Programme).

TOWNSHEND, J.R.G. and JUSTICE, C.O., 1986, Analysis of the dynamics of African vegetation using the normalized difference vegetation index. *International Journal of Remote Sensing*, **7**, pp. 1435–1445.

TRAUTH, M.H., ALONSO, R.A., HASELTON, K.R., HERMANNS, R.L. and STRECKER, M.R., 2000, Climate change and mass movements in the NW Argentine Andes. *Earth and Planetary Science Letters*, **179**, pp. 243–256.

TUCKER, C.J., JUSTICE, C.O. and PRINCE, S.D., 1986, Monitoring the grasslands of the Sahel 1984–1985. *International Journal of Remote Sensing*, **7**, pp. 1571–1581.

VERHOEF, W., 1996, Application of Harmonic Analysis of NDVI Time Series (HANTS). In *Fourier Analysis of Temporal NDVI in the Southern African and American Continents*, S. Azzali and M. Menenti (Eds), pp. 19–24 (Wageningen, the Netherlands: Winand Staring Centre for Integrated Land, Soil and Water Research).

VERHOEF, W., MENENTI, M. and AZZALI, S., 1996, A colour composite of NOAA-AVHRR-NDVI based on time series analysis 1981–1992. *International Journal of Remote Sensing*, **17**, pp. 231–235.